Heat Transfer Measurements of NASA Liquid Kerosene/Oxygen Rotating Detonation Rocket Engine

Thomas Teasley[1], Dillon Petty[2], Michaela Hemming[3]
NASA Marshall Space Flight Center, Huntsville, AL, 35808, United States

David Scarborough[4]
Auburn University, Auburn, AL, 36849, United States

Stephen Heister[5]
Purdue University, West Lafayette, IN, 47906, United States

The RDRE has been identified as a viable high performance propulsion system with numerous advantages over the state-of-the-art (SOA) liquid rocket engine. NASA has been investigating this combustion device for applications ranging from lander, upper stage, thruster, and hypersonics. All of the activities funded to date have been focused on closing major technology gaps preventing the RDRE from being used more broadly by industry. One of those gaps include the prediction and management of heat transfer to the walls from the extreme combustion environment. This work overviews the heat transfer measurements made using new and existing hardware. A liquid oxygen / liquid RP-1 RDRE was tested utilizing a calorimeter outer body and outer body nozzle extension. An actively cooled inner body with axial running cooling channels was also used. A bimetallic GRCop-42 / Monel K500 injector was developed and demonstrated to be a viable technology for RDRE environments. Trends in bulk heat loads are discussed along with a direct comparison to constant pressure theory predictions of wall heat transfer. The experimental data obtained in this investigation showed similar heat fluxes to constant pressure theory indicating deflagration may have dominated the flow field. Only a single detonation wave was observed in all tests which imparted a significant dynamic load (vibration) on the test article making measurement of combustor performances extremely challenging. Both accelerometer and load cell data corroborate the extreme G-forces measured. The single wave mode yielded relatively low performances compared with other hot fire test data sets available. This leads to the conclusion that a single detonation wave in this geometry is not sufficient for high performance. Wave multiplicity, or rather, a specific number of waves may yield higher performances.

I. Nomenclature

AM	=	additive manufacturing
CAD	=	computer aided design
CP	=	constant pressure
CTAP	=	capillary tube attenuated pressure
CASI	=	compact augmented spark igniter

[1] Combustion Devices Engineer, Engine Component Development and Technology Branch, NASA MSFC
[2] Combustion Devices Engineer, Engine Component Development and Technology Branch, NASA MSFC
[3] NASA Space Technology Research Fellow, Engine Component Development and Technology Branch, NASA MSFC
[4] Associate Professor, Auburn University
[5] Raisbeck Professor, Purdue University

*C**	=	characteristic exhaust velocity
DDT	=	deflagration to detonation
DI	=	de-ionized
EHV	=	electrohydraulic valve
GH2	=	gaseous hydrogen
Isp	=	specific impulse
L-PBF	=	laser powder bed fusion
LOx	=	liquid oxygen
LCH4	=	liquid methane
*L**	=	chamber characteristic length (volume / throat area)
L'	=	distance from injector face to throat proper.
MSFC	=	Marshall Space Flight Center
MR	=	mixture ratio
NASA	=	National Aeronautics and Space Administration
PGC	=	pressure gain combustion
RDRE	=	rotating detonation rocket engine
RDE	=	rotating detonation engine
SOA	=	state-of-the-art
TCA	=	thrust chamber assembly
TRL	=	technology readiness level

II. Introduction

As a continued effort to further evaluate critical performances of rotating detonation rocket engine (RDRE) technologies, NASA's Space Technology Mission Directorate (STMD) has funded an early career initiative (ECI) project to close the remaining technology gaps preventing the RDRE from widespread use within the United States. As part of this project, evaluation of heat transfer trends, operability, and critical design features are presented.

The RDRE consists of a ring-shaped chamber that enables a tangential instability to form and accelerate to supersonic speeds rapidly after ignition. This supersonic combustion event, known as a detonation, enables a high-pressure ratio that completes combustion orders of magnitude faster than traditional constant pressure combustion (deflagration). The rapid completion of combustion substantially reduces the annulus characteristic length, L', where many geometries tested to date yield complete combustion within a few inches from the injection plane. Equivalent constant pressure combustion devices would require high "stay times" within the main thrust chamber with L' values on the order of dozens of inches to a few feet. A major consequence of rapid combustion is higher combustion temperatures, lower ratios of specific heat, and thus higher overall specific impulse. The inherent ring geometry allows for the inclusion of a plug or aerospike nozzle on the interior in addition to a shroud or bell like nozzle on the exterior. Combustion products can then expand against the two surfaces at the same time allowing for substantial reductions in nozzle length. Overall, the length trades for an RDRE have been found to be staggering from a systems perspective. One major requirement of the RDRE due to the higher combustion temperatures, is the use of additive manufacturing (AM) and specialized alloys such as GRCop-42 and GRX-810. Many of the complex integrated structures such as coolant channels, flow paths, and instrumentation ports are extremely difficult if not impossible to traditionally manufacture. Survivability of hardware at flight realistic operating conditions also hinges on the use of these extreme environment alloys.

Under this investigation, a fully additively manufactured laser powder bed fusion (L-PBF) GRCop-42 alloy calorimeter chamber was manufactured and tested with liquid kerosene and liquid oxygen direct injection. All chamber hardware was actively cooled using de-ionized water. The hot wall contour closely matched that of case 3 in Fig. 13 of [1], [2] to better evaluate global performance metrics such as thrust. A major finding of this work corroborates the computational results of [1], [2] where a nozzle shroud extending past the geometric throat from the outer body yields significantly higher thrust and Isp than a baseline configuration with no nozzle shroud. The primary focus of this work is to provide insights into heat transfer trends at an elevated thrust class. However, the additional discovery of extreme vibratory loads with a single wave mode is also a major finding of this effort. Images of pivotal hot fire tests conducted under this ECI project since 2023 are shown in Fig 1.

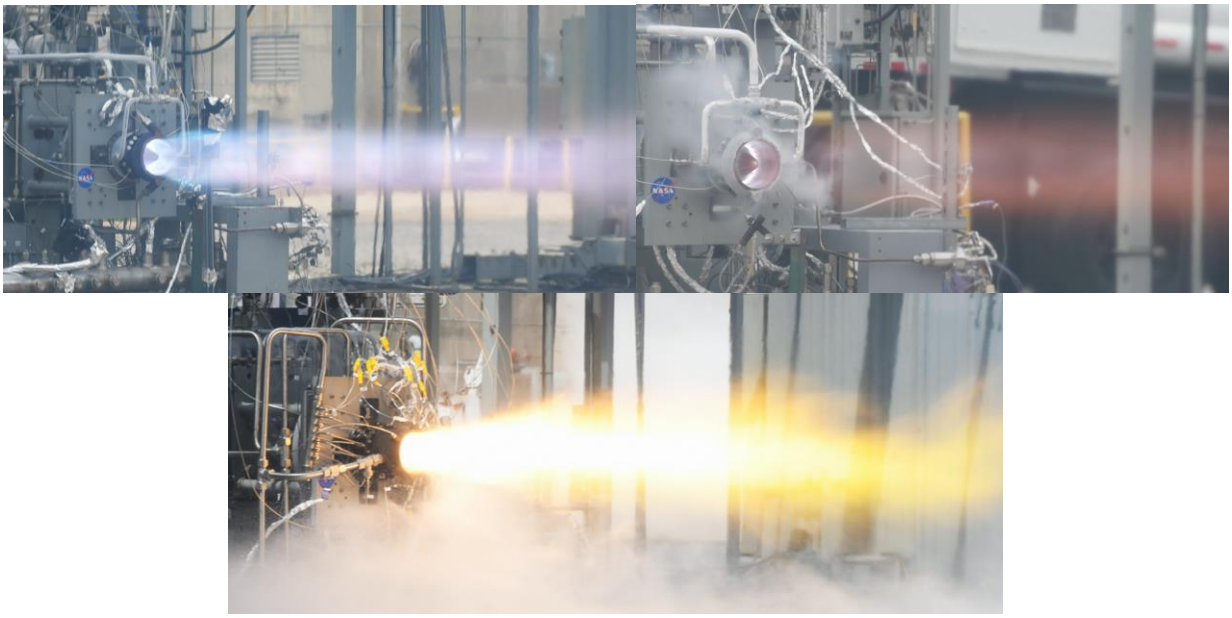

Fig 1. NASA RDRE pivotal hot fire tests using methane/oxygen (top left), hydrogen/oxygen (top right), and RP1/oxygen (bottom).

Several major design parameters, identified from experimental data, have shown to have direct impacts on combustor performance outcomes. These performances include specific impulse, total heat loads and heat fluxes, and nozzle thrust coefficient. The success of this experimental work has also shown mission performance advancements involving hardware cost, mass, and schedule improvements. The geometry presented in this work did not implement many of these critical design parameters since it was developed prior to their discovery. New hardware has since been manufactured and tested in the late summer of 2024 showing dramatic improvements in performances over this current geometry. Images of the kerosene hardware as installed in the test stand at Marshall's heritage East Test Area (test stand 115) are shown in Fig 2 and during depowdering in Fig 3.

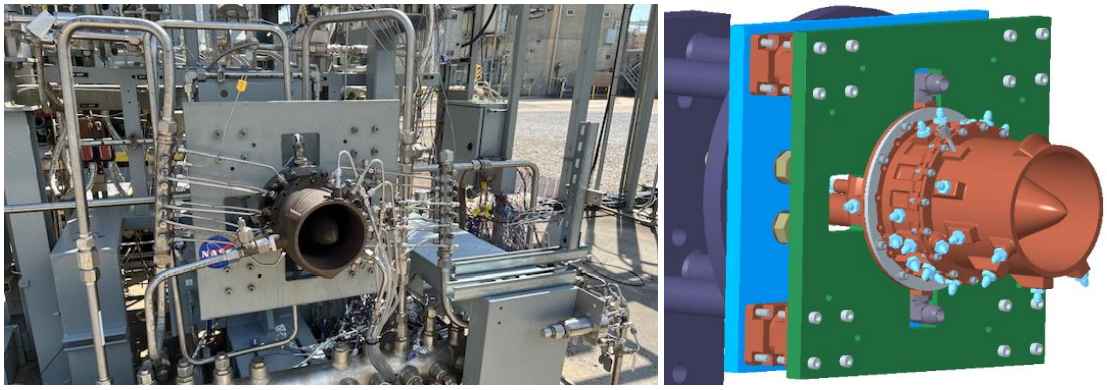

Fig 2. V1 calorimeter RDRE (left) and V3 CAD RDRE (right) as built-up on the TS115 stand.

Fig 3. Kerosene RDRE GRCop-42 inner body (left) and outer body calorimeter nozzle extension (right) during the depowdering process.

A. Chamber, Injector, and Igniter Hardware

All chamber and injector hardware were produced using L-PBF GRCop-42 (Cu-4Cr-2Nb) as it has potential to withstand high pressure detonative environments given its high strength at substantial hot wall temperatures [3]–[5]. Each individual component was fabricated at a select additive powder bed fusion vendor within the US. Table 1 lists pertinent design features of the annular chamber.

Table 1. Summary of Chamber Geometry

L", Overall length to nozzle exit (in)	9.00
L', length from injector face to throat (in)	4.00
Inner Body Diameter (in)	5.59
Outer Body Diameter (in)	6.25
Annulus Gap Width G_c (in)	0.33
Expansion Ratio, A_e/A_t	6.30
Subsonic Area Ratio, A_{inj}/A_t	1.25

This geometry has been found to be non-ideal for direct liquid injection of RP-1/Liquid Oxygen. In addition, this investigation was an initial step towards evaluating large scale Kerosene RDRE designs. The use of non-heated liquid injection would likely be reserved to an ablative chamber design, but the combination does theoretically provide the highest performance detonation conditions [6]. More practical designs would regeneratively cool hardware with the propellant and inject in a heated or conditioned state. Oxygen rich staged combustion cycles, for example, may require gas injection temperatures up to 1400 F which would dramatically change the detonative response of the combustor.

The coolant channel geometry for the inner body was designed explicitly using previously obtained NASA lessons learned from methane hot fire calorimetry data. However, overcooling with water is a major advantage for experimental work that is uncertain of specific heat flux contours subjected to hardware. Furthermore, the coolant channel geometry was designed specifically to the maximum allowable pressure budget of the facility rather than to meet a specific hot wall temperature.

Each injector was designed using typical element schemes with appropriate pressure losses to combat backflow. Many of the considerations implemented into the injector design were specific to additive manufacturing requirements and targeted obtaining correct discharge coefficients. Printed orifices will not have typical discharge coefficients, and are generally lower than anticipated values, since they include shrinkage and roughness factors incorporated. Details on the injector design specifics will be shared at the upcoming JANNAF conference or by request from ITAR qualified individuals. The primary injector tested consisted of a GRCop-42 injector face and bimetallic L-PBF body made of Monel K500. This design was manufactured in partnership with Quadrus Corp. under an existing SBIR phase 2 effort. An image of the injector is shown in Fig 4.

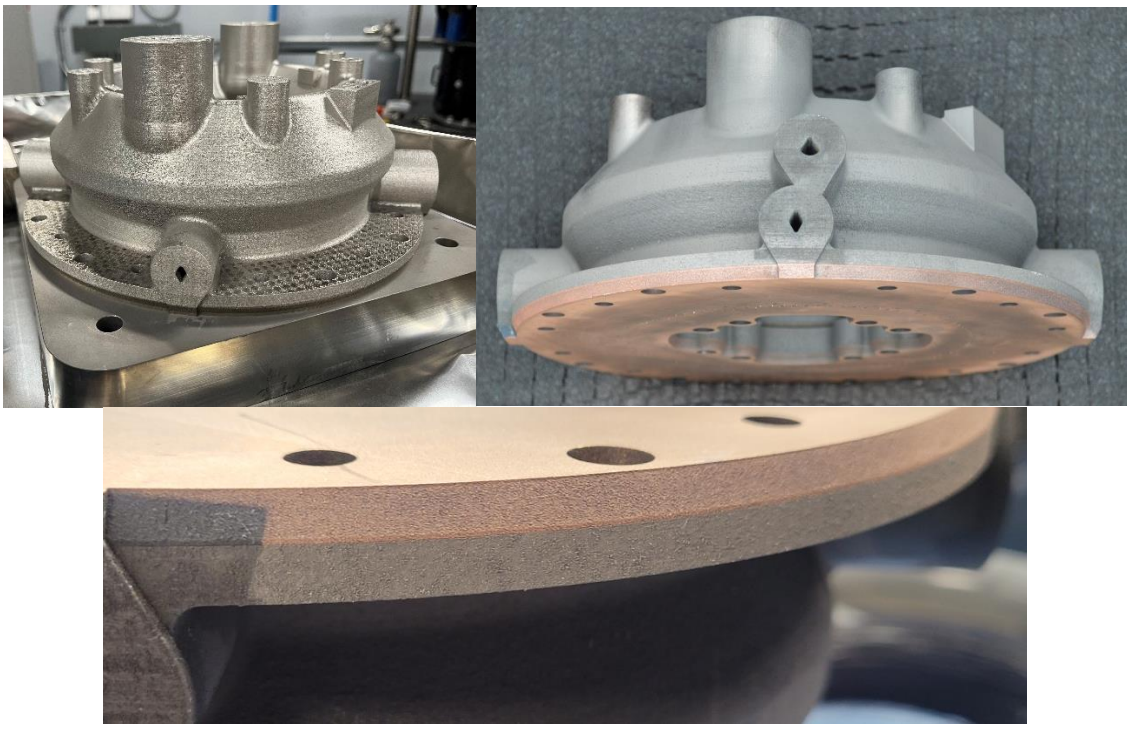

Fig 4. Bimetallic L-PBF (GRCop-42 and Monel K500) RDRE injector.

The specific combination of GRCop-42 and Monel K500 was chosen to enable survival of the injector face in an extreme combustion environment while the injector body would need to survive a high oxygen content environment. The injector survived all tests and operating environments, thus proving out the technology and elevating its TRL from a 2 to a 3. The injector face did not show any indication of heat staining and likely could have survived hot fires with a thinner layer of GRCop-42, further reducing cost and weight of the device.

An integrated variant of NASAs compact augmented spark impinging (CASI) igniter previously used under nearly a dozen other NASA test projects since 2019 [7]–[11] was modified for use with TEA/TEB and nitrogen. Nitrogen was specifically used to aid in the atomization and distribution of TEA/TEB with the CASI igniter manifold to avoid overfilling the manifold with an excess of the pyrophoric fluid. The primary reason for using TEA/TEB as opposed to the augmented torch igniter was to guarantee ignition. Ignition has been found to be challenging for RDREs since the "stay time" of propellants within the annulus is an order of magnitude lower than cylindrical rocket chambers.

III. Experimental Design

The propellant used in this investigation were liquid kerosene (RP-1) and liquid oxygen for tests 001 and 002. Test 003 utilized a Kerosene alternative fuel whose data will be shared at the upcoming JANNAF conference. Kerosene was injected at ambient conditions (~70 F) while liquid oxygen typically entered the injector manifold at about -250 F/120K on average. A wide range of total mass flow rates were explored yielding a large range of capillary tube attenuated pressures (CTAP) within the annulus specifically at the injector face, geometric throat, and nozzle exit plane. Only 3 hot fires were achieved with several throttle points evaluated within each hot fire. A plot of the mean chamber pressure and mixture ratios explored are shown in Fig 5.

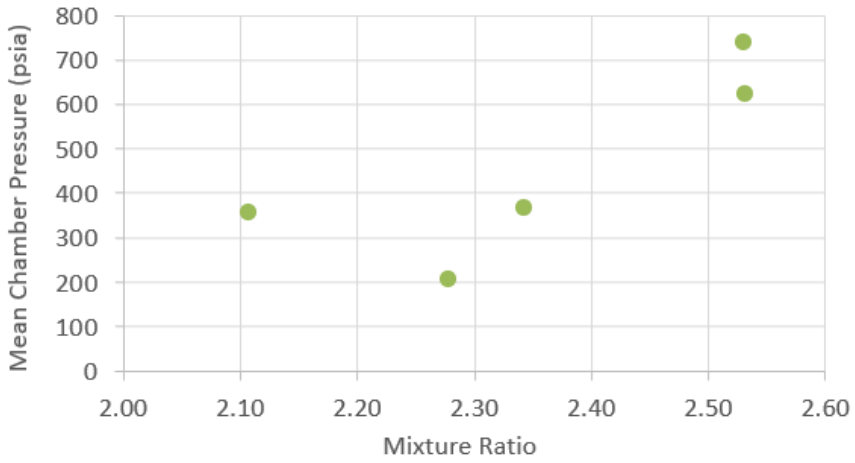

Fig 5. Mean chamber pressure (CTAP) at the injection plane as a function of mixture ratio.

In all cases, only a single detonation wave was observed. Dynamic loads, more specifically vibrations, on the hardware were extreme causing the failure of a machined mating groove on the back side of the inner body thus leaking water into the annulus during test 002. The inner body was then repaired with a weldment of copper alloy rod and re-machined. The third hot fire burned through several coolant channels on the inner body and ultimately was discovered that weldment had blocked off several coolant channels in posttest evaluation. Regardless, a sufficient range in total mass flow rate and mixture ratio was explored to inform the investigators that only the single wave mode could be achieved with this current design. Subsequent testing would only have caused further damage to the test stand and hardware from the extreme vibrational environments.

IV. Discussion of Results

Hot fire testing was conducted over the course of a week at Marshall Space Flight Centers TS115. High speed videography in conjunction with external microphones were used to ascertain wave behavior. Water cooled calorimetry hardware obtained accurate measurements of wall heat fluxes as a function of axial length and piezoelectric triaxial load cells obtained direct measurements of thrust. Accelerometer data corroborated the measured vibrations from the load cell data.

A. Wave Activity and Performance

In all hot fire tests conducted, only a single strong detonation wave was observed. The dynamic vibrations imparted on the thrust structure and hardware were so extreme that multiple torqued fittings backed out, bolts loosened, and instrumentation failed. To illustrate the range in dynamic forces, a plot of the measured thrust as a function of time from test 001 is shown in Fig 6 showing large amounts of noise during the hot fire interval between 60 and 66 seconds. The mean Z axis thrust is also plotted in red.

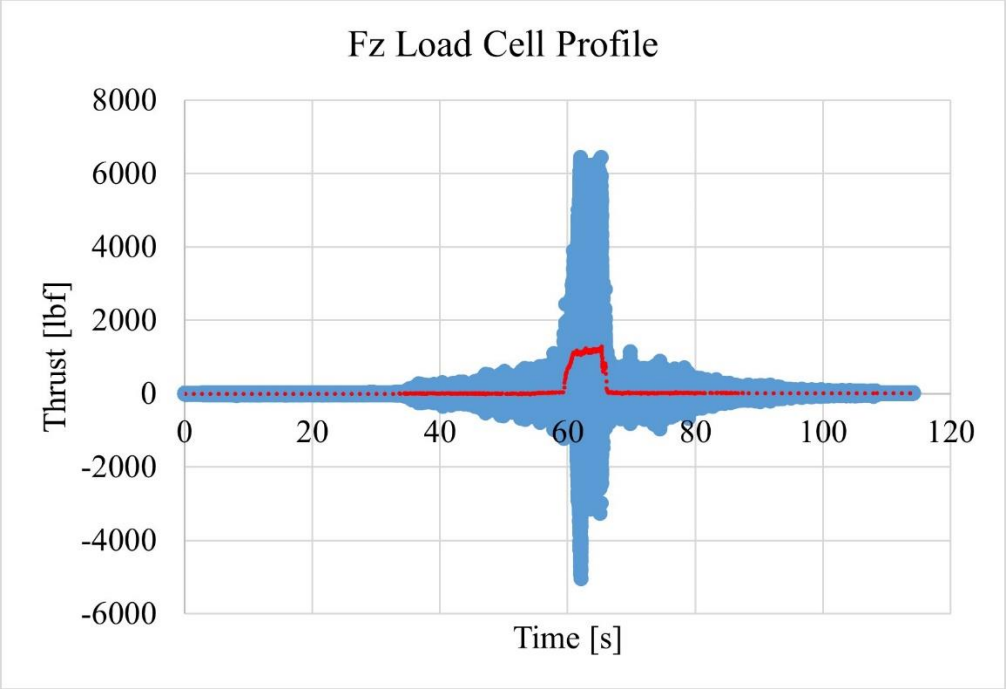

Fig 6. Z-axis thrust measurements capturing dynamic forces imparted on the thrust structure during hot fire from the single wave modes.

Accelerometer data corroborated these measurements with over 1000 G's measured, clipping the measurement capability of the sensor. The min to max force was found to be greater than 11,000 lbf for this test case with tests 002 and 003 clipping the measurement capability of the load cells. Accelerometer data is presented in Fig 7.

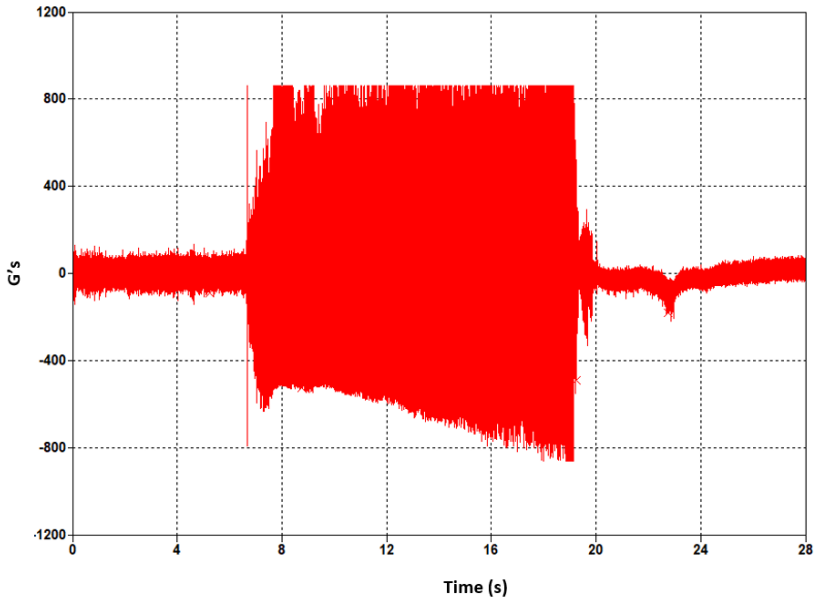

Fig 7. Accelerometer data for test 002 in the Z axis of thrust, G Force as a function of time (seconds).

These data show clipping of the accelerometer's measurement capability at about 850 G's with the bulk of forces measured in the Z axis. An image of the clockwise rotating detonation from test 002 is shown in Fig 8.

Fig 8. Images of test 002 clockwise rotating detonation from high-speed video.

Because the thrust class of this test article is in the 1000-10,000 lbf range, the high-speed camera had to be offset from the centerline of thrust. Thus, only a portion of the annulus could be observed in each test without irreparable damage to the high-speed camera.

Wave speeds were found to increase with increasing total mass flow rate. This behavior has been observed previously in open data sets and other NASA hardware. The highest wave speed found in test 002 was measured to be just under 4200 ft/s at a mean chamber pressure of about 360 psia. In all test cases, with the exception of test 001, the wave direction was clockwise. The wave direction did not appear to impact heat flux profile or other performance metrics.

Two high frequency microphones were used to capture the acoustic environments exterior to the test article. They were mounted approximately 3 feet off to the side of the combustor. The measured sound pressure level was found to exceed about 175 dB at the peak with a root mean square (RMS) value as high as 170 dB at ignition. The power spectral density showed two major peaks at 2.15K Hz and 6.43 K Hz. The former matched the rotating frequency of the single wave mode confirmed via high-speed videography. The latter is likely the second harmonic resonating with the thrust structure as no underlying activity outside of the primary single wave mode was observed in the high-speed data. These data are shown in Fig 9.

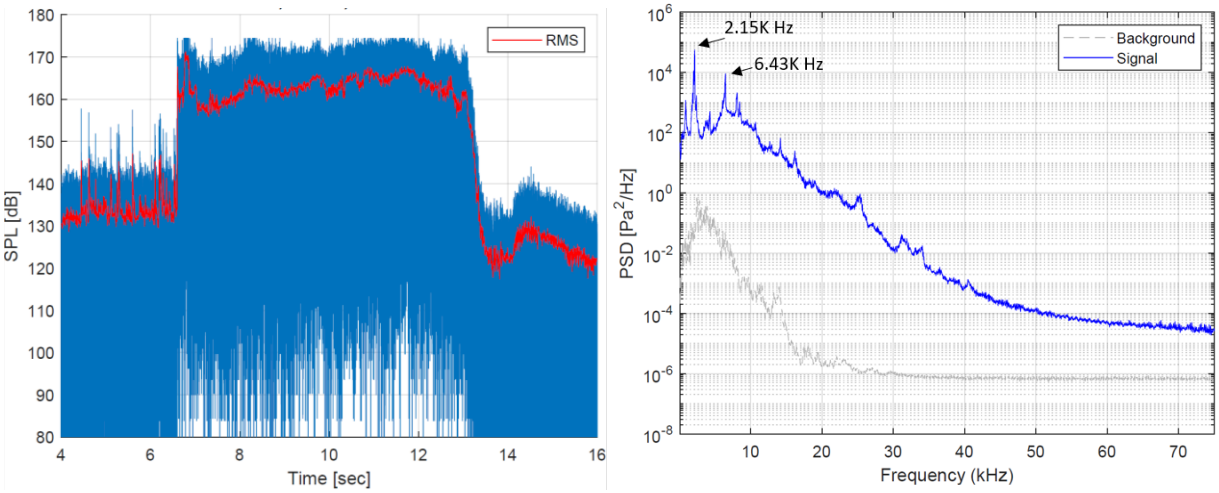

Fig 9. Sound pressure level and power spectral density plots for test 001.

B. Wall Soot and TEA-Ash Observations

Heavy wall soot and TEA-ash buildup was observed on the hot wall post tests 001 and 002. Heavy soot formation within the plume was observed and is characterized by the typical bright yellow exhaust with some green hues from burned TEA/TEB. TEA-ash is characterized by white buildup on the hot wall. Images of the test articles post hot fire are shown in Fig 10.

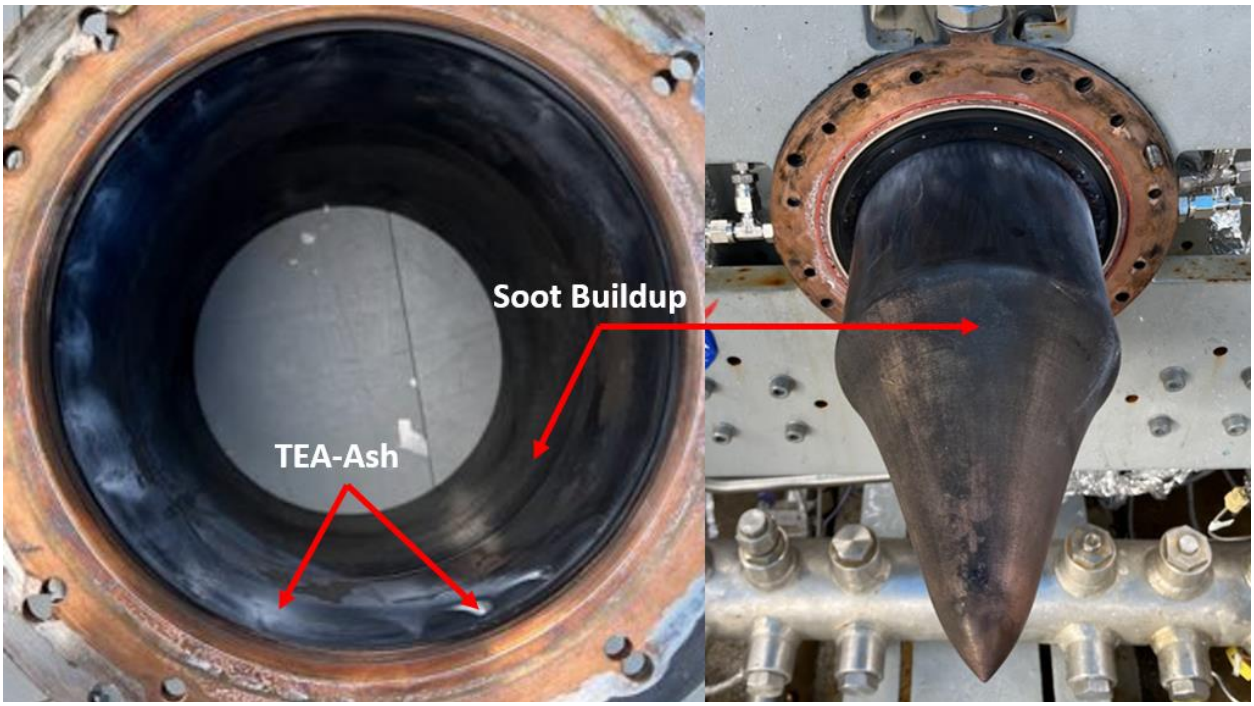

Fig 10. Post test 002 images of the outer body and inner body hot walls with substantial soot and TEA-ash buildup.

Previous hot fire testing of combustion device hardware has shown the buildup of soot and TEA-ash can reduce overall wall heat loads by anywhere from 10-40% depending on the severity [12]. The buildup on the hot wall of these hardware suggests a 25% reduction based solely on hot fire test experience of the test requesting engineers. Under the previously mentioned CIF work with Purdue University, the hardware geometry and injection conditions tested enabled multi-mode operation with very little wall soot buildup. Images of these hardware post several dozen tests are shown in Fig 11.

Fig 11. Purdue/NASA CIF hardware post dozens of hot fire tests courtesy of Dr. Ariana Martinez from [13]**.**

A stark difference in plume coloration was observed between these two test articles. A lack of soot formation was observed with the CIF hardware yielding a purple/blue plume. Images comparing these hardware hot fires are shown in Fig 12.

Fig 12. Purdue/NASA CIF hardware [13] **(left) and NASA ECI hardware (right) during hot fire.**

Ultimately, soot formation may be considered an indication of lower efficiency combustion while a lack of soot in the plume may indicate reduced combustion time scales inhibiting soot formation. Further investigation is needed to better understand this phenomenon. Both test articles likely represent the extreme ends of the design space where an ideally performing Kerosene RDRE may exist.

C. Heat Transfer Measurements

The heat transfer to the walls of the inner and outer bodies was obtained by calculating the change in enthalpy to the coolant and multiplying by the total mass flow rate of coolant. In most cases below, these data are presented as a function of measured injection plane pressure. In the majority of cases, the severity of vibrations from the detonation wave caused significant error in the measurement of coolant inlet and exit temperature and pressure. Only once the combustor was shutdown were the measurements able to reestablish meaningful values and yield reliable data. All data presented in this section were obtained in this fashion prior to the coolant temperature reducing in the ramp down of coolant mass flow rate at the end of each test. Fig 13 and Fig 14 show the measured total heat load and mean heat flux, respectively, to the coolant as a function of the measured injection plane pressure.

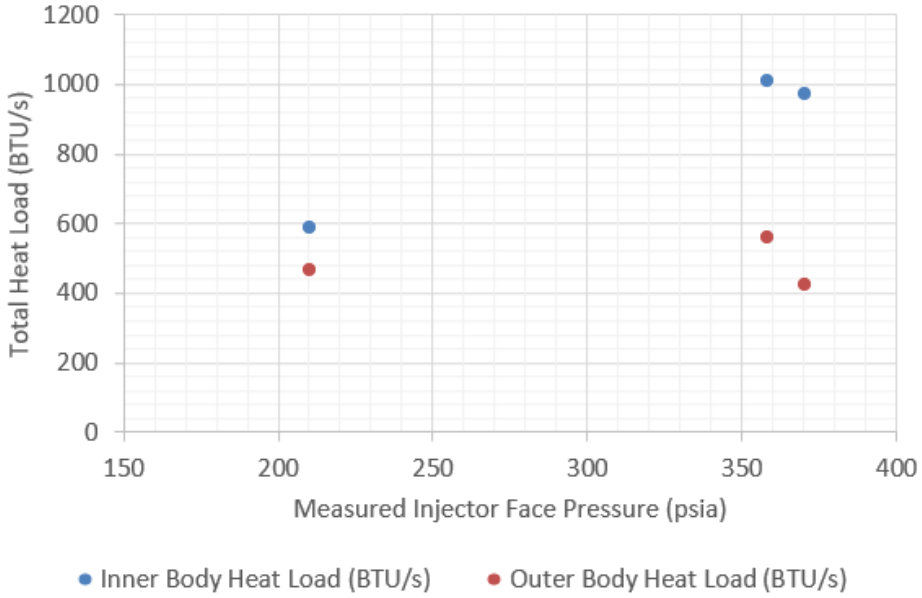

Fig 13. Total heat load to the inner body and outer body as a function of measured injection plane pressure.

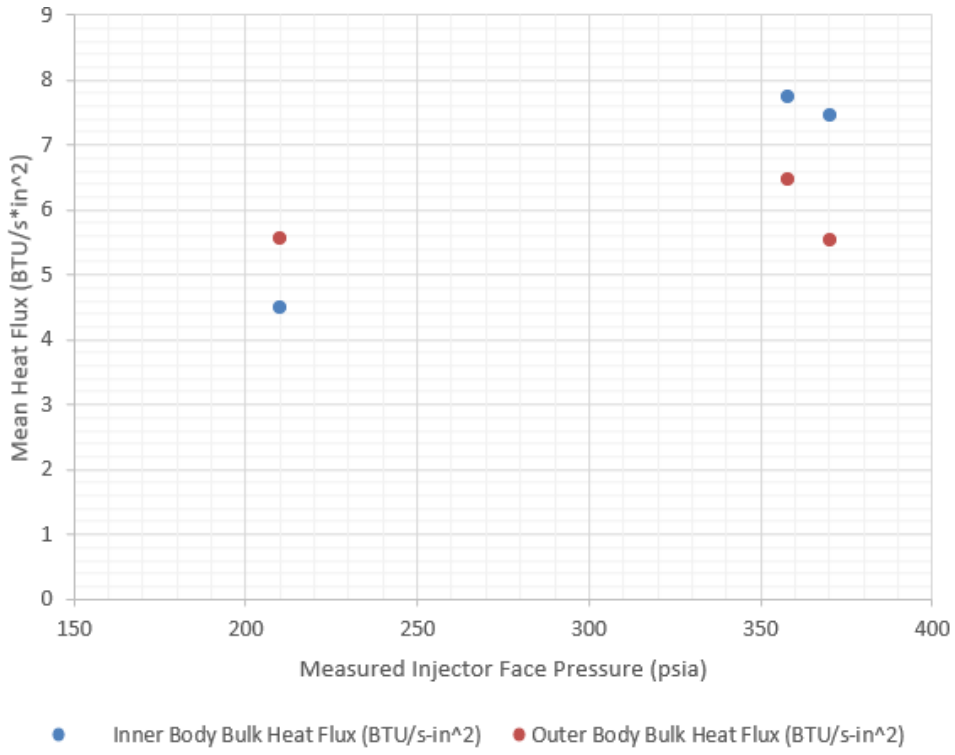

Fig 14. Mean wall heat flux to the inner body and outer body as a function of measured injection plane pressure.

The inner body included the heat addition to the plug nozzle however, it is estimated that this proportion of heat addition likely contributes less than 8% of the total heat input, even though surface area is approximately 35% of the component. This is entirely due to low on average heat flux in the expansion section of the nozzle relative to the annulus. In addition, the influence of leaking water into the annulus during hot fires 002 and 003 likely are introducing error in the quantities presented. However, it is unknown what this error may be. The measurements from the calorimetry outer body and nozzle extension captured usable trends in the heat flux shown in Fig 15.

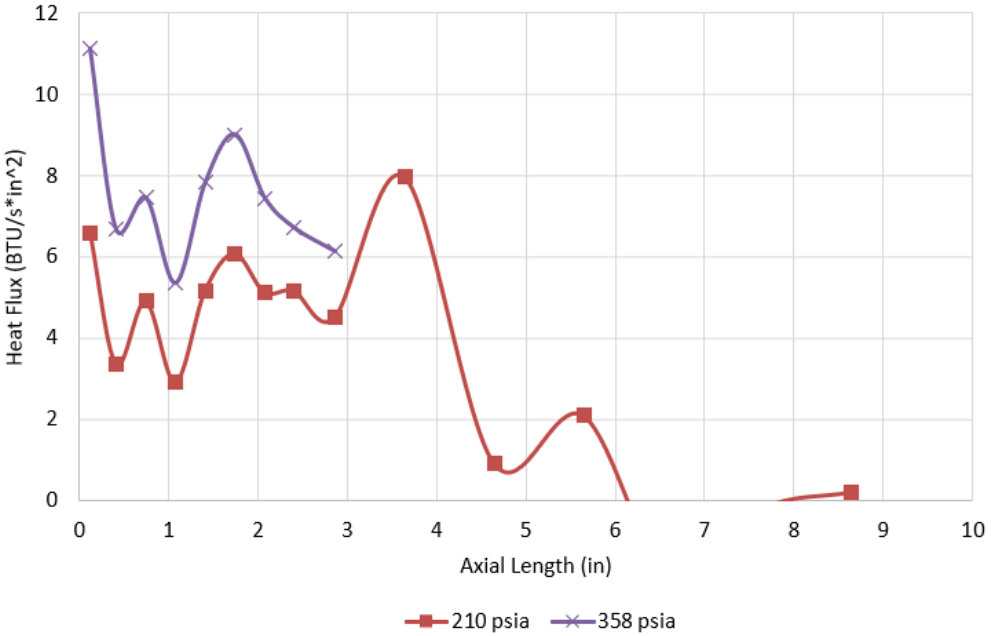

Fig 15. Heat flux profile as a function of axial length for varying injection plane pressures.

These data show a large jump in the heat flux at the injection plane where the detonation wave resides, followed by a plateau and an abrupt rise where the throat area contraction is, located at +4 inches. Note that the thermocouples from X = 3" and further for test 002 did not yield data of value. Those thermocouple data were not recoverable. Generally, this profile resembles what was expected and looks like other experimental data sets in the open and closed experimental literature. Note that a single data point was found to read a negative heat flux at approximately 6.5 inches from the injection plane. This is nonphysical and illustrates the impact of high error in these measurements. However, attempts at scaling these data at each axial location does not match the more reliable data sets NASA currently has. This was also expected given that hardware leaks, dynamic vibrations from the detonation, and uneven wall soot and TEA-ash buildup are likely imparting substantial error. The wall heat fluxes presented are much lower compared with data presented by [13] with NASA/Purdue CIF RP/GOx hardware and substantially lower than high performing methane/oxygen NASA hardware. Regardless, these data further illustrate the need for corroborating data from the pressure gain combustion community.

To further evaluate these data, direct comparison to constant pressure theory throat level heat fluxes was conducted. The throat level heat flux was computed using Bartz heat flux correlation assuming frozen chemistry [14]. It is well known that Bartz throat level heat flux dramatically overpredicts the true heat flux a constant pressure rocket experiences. This is likely a combination of error in calculating the Nusselt and Prandtl numbers along with reduced wall static pressure as the combustion products accelerate at the throat. This is particularly the case for Kerosene engines as the slow chemical kinetics and wide-ranging combustion species formed in the reaction tend to reduce overall combustor efficiency compared to simplification of constant pressure theory. In addition, the soot buildup on the walls of the test article likely insulated and reduced the measured heat flux further. The computed Bartz throat level heat flux as a function of mean chamber pressure is shown in Fig 16. In addition, the ratio was taken between the measured injection plane and throat heat fluxes to the computed Bartz throat heat flux also shown in Fig 16.

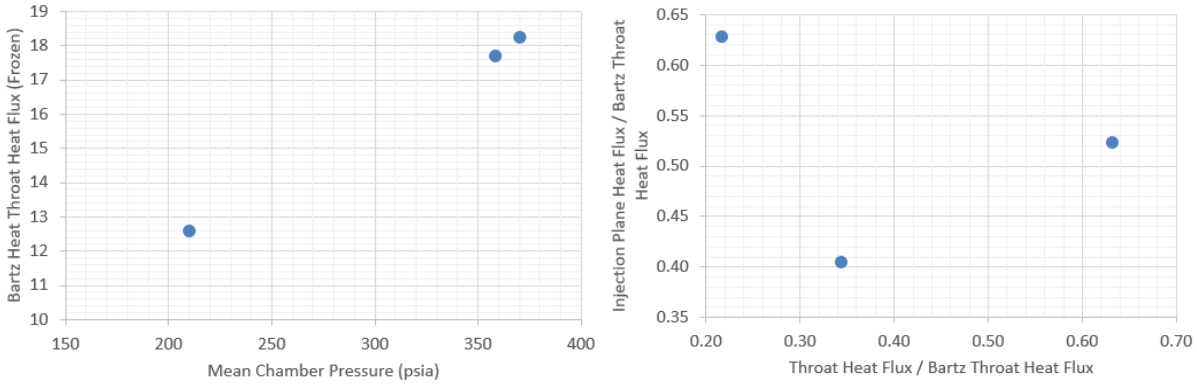

Fig 16. Bartz predicted throat level heat flux (frozen chemistry) as a function of mean chamber pressure (left) and ratio of the injection plane heat flux to Bartz throat heat flux as a function of the measured throat heat flux to Bartz throat heat flux (right).

The ratio of measured to predicted throat heat flux is also plotted as a function of mean chamber pressure in Fig 17.

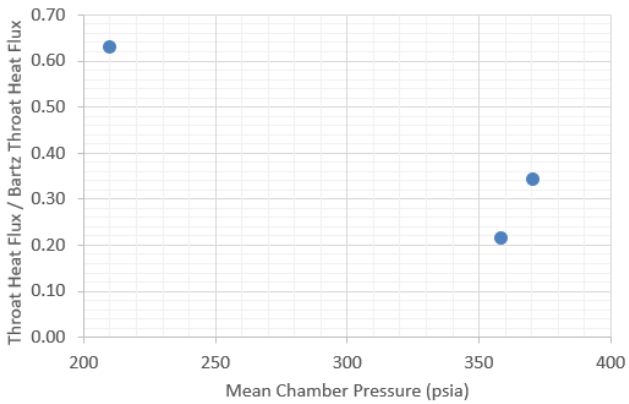

Fig 17. Ratio of measured throat heat flux to Bartz throat heat flux as a function of mean chamber pressure.

This analysis and data is limited but some inferences can be made. It appears that the throat heat flux widely varies while the injection plane heat flux where the detonation resides appears to average around 50%. From other data sets, it is known that the injection plane heat flux is at least an order of magnitude higher for high performing methane RDREs. In addition, the throat heat flux ratio has been observed to be more than double the predicted value. With that said, this configuration is likely just a low performing RDRE relative to other designs tested. It is known how to improve this design going forward to achieve markedly higher performance, details of which will be shared at upcoming JANNAF conferences.

D. Combustion and Specific Impulse Measurements

Of the more reliable data considered, the overall combustion efficiency and Isp efficiency were found to be high for a Kerosene combustor. The highest measured thrust achieved in this test project was about 5300 lbf at a mean chamber pressure of about 740 psia and an Isp of 246 seconds. Most public information on Kerosene constant pressure rockets show that the best C* and Isp efficiencies are around 96% and 92%, respectively. The RD-180 operating close to 4000 psia, yields an Isp efficiency of about 96.6% assuming frozen chemistry, and 91.5% assuming equilibrium chemistry, though likely there are better performing devices in the closed literature. The data obtained from this hardware yielded the highest Isp efficiency of 95% and combustion efficiency of 86% assuming equilibrium chemistry, and it is already known that this hardware is low performing relative to other data sets NASA currently has. For a constant pressure kerosene engine, it is typical to obtain Isp and combustion efficiencies between 80-90% from the first design iteration.

Subsequent design revisions often yield better performance in excess of 90% (frozen chemistry). Fig 18 shows the trend in Isp efficiency as a function of combustion efficiency and suggests a mismatch in the measured quantities from what is expected. Further evaluation of these data are needed to understand the complex interplay between the pressure environment and force generated from an unsteady combustion device such as an RDRE. Data has already been obtained from subscale RDREs tested at Marshall Space Flight Center that will document and make further sense of this relationship.

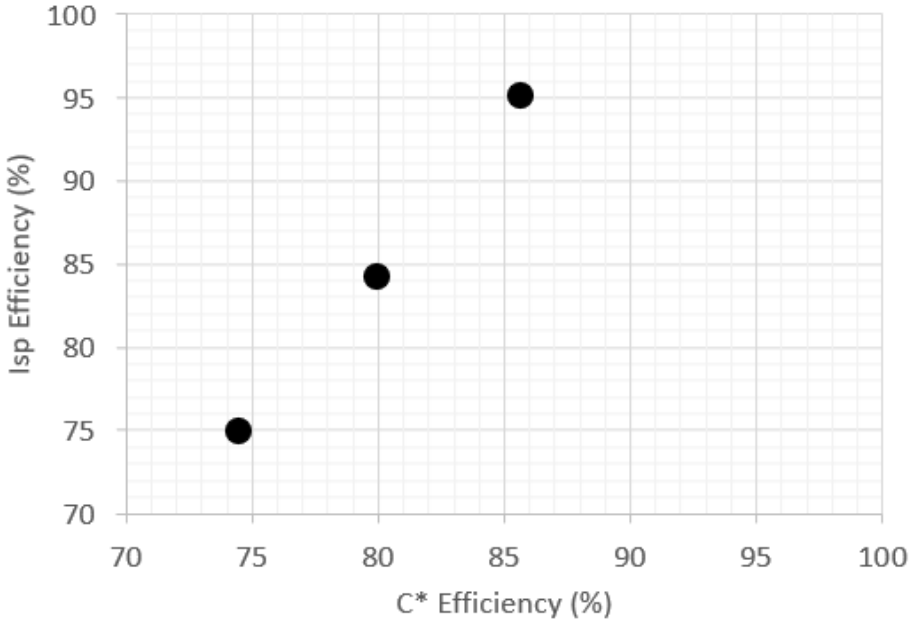

Fig 18. Isp efficiency as a function of combustion efficiency for several RDRE hot fires.

Finally, the ratio of the nozzle exit pressure and the throat total pressure were evaluated against the ideal calculated quantities. It is expected that a constant pressure rocket may yield values that are slightly less than 1 due to cumulative losses. However, the RDRE measured values similar to or greater than the ideal calculated values shown in Fig 19.

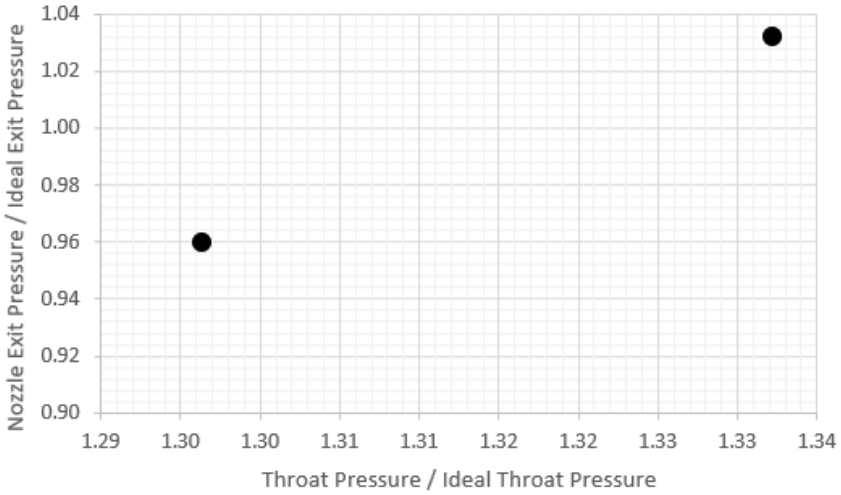

Fig 19. Ratio of the measured nozzle exit pressure and throat total pressure to the ideal calculated quantities.

These measurements are not in isolation as direct measurements on different scale RDREs have also been measured with similar results. While it is not clear what this means as of yet, it is expected that an inherently unsteady

combustor may yield elevated total pressures since heat release is expected to be higher than a constant pressure rocket.

V. Summary and Conclusions

The data presented in this work is limited by test challenges brought on by the extreme combustion environments of large scale RDRE testing. However, it lays the groundwork towards addressing the heat transfer challenges of Kerosene RDREs and builds off of previous hot fire success conducted at Purdue University. These data are only an introduction to a single data set in a planned database of heat transfer results. Liquid/liquid, liquid/gas, and gas/gas heat transfer data will be obtained over the course of the next year. Subscale and full-scale hardware will be tested with variation on injector design, contraction ratio, and annulus length to fully capture the impact of heat transfer variation in these unsteady combustors. In addition, academic and industry partners will be exploring validation cases with different propellants, phases, and injection temperatures in the near future.

This study evaluated a direct injection (liquid/liquid) Kerosene (RP1)/Liquid oxygen RDRE. Mean chamber pressures from about 210 psia to 740 psia were explored. Direct measurement of heat fluxes were made in the outer body and bulk heat loads in the inner body. Test related challenges such as wall sooting and TEA-ash buildup along with high vibrational loading from the single wave mode limited the accuracy of measured heat transfer parameters. However, these data bound other existing and higher performing data sets establishing critical design criteria for RDREs.

Future Work

Much of the future work planned for heat transfer measurements and computational activities involve the use of NASAs full scale and subscale hardware. To date, calorimetry data has been obtained at mean chamber pressures up to 1250 psia with plans to evaluate heat flux up to 1800 psia with both kerosene and methane fuels.

Acknowledgments

This work is funded by the NASA Space Technology Mission Directorate (STMD) through an early career initiative (ECI) project.

References

[1] K. Miki, D. E. Paxson, D. Perkins, and S. Yungster, "RDE Nozzle Computational Design Methodology Development and Application," in *AIAA Propulsion and Energy 2020 Forum*, 2020, p. 3872.

[2] D. E. Paxson, K. Miki, H. D. Perkins, and S. Yungster, "Computational Fluid Dynamic Optimization of an Experimental Rotating Detonation Rocket Engine Nozzle," in *AIAA AVIATION 2022 Forum*, 2022, p. 4107.

[3] P. R. Gradl, T. W. Teasley, C. S. Protz, C. P. Garcia, and S. E. Greene, "Hot-fire Performance of Additively Manufactured GRCop-42 and GRCop-84 Channel-Cooled Combustion Chambers," pp. 1–36, 2019.

[4] D. L. Ellis, "GRCop-84: A high-temperature copper alloy for high-heat-flux applications," 2005.

[5] T. W. Teasley, P. R. Gradl, M. B. Garcia, B. B. Williams, and C. S. Protz, "Extreme Environment Hot Fire Durability of Post Processed Additively Manufactured GRCop-Alloy Combustion Chambers," in *AIAA Propulsion and Energy 2021 Forum*, 2021, p. 3233.

[6] A. Harroun and S. D. Heister, "Liquid Fuel Survey for Rotating Detonation Rocket Engines," in *AIAA SCITECH 2022 Forum*, 2022, p. 0088.

[7] S. E. Greene, "Test Summary Report for PJ030: Modified Methane Engine Thrust Assembly for 4K lbf with a 4" Diameter Chamber (META4X4)," Huntsville, AL, 2020.

[8] T. W. Teasley, "Test Summary Report for Test Program PJ062 "1.2K GRCop Chamber and HR-1 Nozzle Cycle Testing"," Huntsville, AL, 2021.

[9] T. W. Teasley and P. R. Gradl, "PJ116 Test Summary Report - Composite Overwrap Methane Engine Thruster (COMET) GRCop-42 7K lbf LOX/Methane Testing," Huntsville, AL, 2021.

[10] T. Teasley, "Test Summary Report for PK129: Cycle Testing of GRCop-42 Long Life Additively Manufactured Assembly (LLAMA) 7K lbf Phase 2," Huntsville, AL, 2021.

[11] T. Teasley, "Test Summary Report for Test Program PK058 & PK129 "Cycle Testing of 7K lbf GRCop-42 Long Life Additively Manufactured Assembly (LLAMA)"," Huntsville, AL, 2021.

[12] T. W. Teasley, "Test Summary Report for Test Program PJ062 "1.2K GRCop Chamber and HR-1 Nozzle Cycle Testing"," Huntsville, AL, 2021.

[13] A. Martinez, B. Cabot, K. Blong, T. W. Teasley, and S. D. Heister, "Experimental Study of a Watercooled GOX/RP-1 Rotating Detonation Rocket Combustor for Application to Ox-Rich Staged Combustion Engine Cycles," in *AIAA SCITECH 2024 Forum*, 2024, p. 2791.

[14] D. H. Huang and D. K. Huzel, *Modern engineering for design of liquid-propellant rocket engines*. American Institute of Aeronautics and Astronautics, 1992.